EUROPEAN **S**YNCHROTRON **R**ADIATION **F**ACILITY

INSTALLATION EUROPEENNE DE RAYONNEMENT SYNCHROTRON

Experiment Report Form

The double page inside this form is to be filled in by all users or groups of users who have had access to beam time for measurements at the ESRF.

Once completed, the report should be submitted electronically to the User Office using the **Electronic Report Submission Application:**

http://193.49.43.2:8080/smis/servlet/UserUtils?start

Reports supporting requests for additional beam time

Reports can now be submitted independently of new proposals – it is necessary simply to indicate the number of the report(s) supporting a new proposal on the proposal form.

The Review Committees reserve the right to reject new proposals from groups who have not reported on the use of beam time allocated previously.

Reports on experiments relating to long term projects

Proposers awarded beam time for a long term project are required to submit an interim report at the end of each year, irrespective of the number of shifts of beam time they have used.

Published papers

All users must give proper credit to ESRF staff members and proper mention to ESRF facilities which were essential for the results described in any ensuing publication. Further, they are obliged to send to the Joint ESRF/ ILL library the complete reference and the abstract of all papers appearing in print, and resulting from the use of the ESRF.

Should you wish to make more general comments on the experiment, please note them on the User Evaluation Form, and send both the Report and the Evaluation Form to the User Office.

Deadlines for submission of Experimental Reports

- 1st March for experiments carried out up until June of the previous year;
- 1st September for experiments carried out up until January of the same year.

Instructions for preparing your Report

- fill in a separate form for each project or series of measurements.
- type your report, in English.
- include the reference number of the proposal to which the report refers.
- make sure that the text, tables and figures fit into the space available.
- if your work is published or is in press, you may prefer to paste in the abstract, and add full reference details. If the abstract is in a language other than English, please include an English translation.

ESRF	**Experiment title:** Synchrotron x-ray diffraction study of the circum corneal annulus of collagen fibrils in the human limbus and its integration with the cornea in normal and pathological	**Experiment number**: WT11
Beamline:	**Date of experiment**: from: 21 mai 02 to: 22 mai 02	**Date of report**: 11 Aug 03
Shifts:	**Local contact(s)**: Dr. Christian RIEKEL	*Received at ESRF:*

Names and affiliations of applicants (* indicates experimentalists):

K. Meek, Cardiff University

H. Ahamohammadzadeh*

C. Boote*

A. Quantock*

Report: (Section of review paper **The Organisation of Collagen in the Corneal Stroma**

Keith M. Meek and Craig Boote (Exp. Eye Res., 2003, In Press))

Abstract

The cornea has evolved to fulfil the dual functions of enclosing and protecting the inner contents of the eye, and focussing light onto the retina with minimum scatter and optical degradation. It does this by means of the arrangement of the constituent collagen fibrils, an arrangement that is unique in connective tissues. This article reviews our current knowledge about the detailed organisation of collagen in the corneal stroma, and presents new data suggesting that a significant proportion of collagen fibrils running across the cornea, change direction near the limbus and fuse with the circumferential limbal collagen.

Methods

The micro-focus x-ray beamline ID-13 at the European Synchrotron Radiation Facility (ESRF, Grenoble), was used to examine in detail the collagen fibril orientation in the final 1-2 mm of tissue before the limbus in human cornea. A whole 68-year old normal left human cornea was used for the study. A suture made in the sclera at time of excision marked the superior position. The fine-focus capability of ID-13 enabled us to sample a circular 5 micron diameter region of the cornea for each data point, with the x-ray exposure time per point being 20s. A translation stage interfaced with the x-ray camera shutter allowed the specimen to be moved in the plane of the cornea between exposures.. Small-angle diffraction patterns were recorded at 1mm intervals along the nasal semi-meridian and also along the supero-temporal semi-meridian. In addition, the final 1mm region of tissue up to the limbus along the nasal semi-meridian was examined at 25 micron intervals, while the final 2 mm was examined at the same resolution on the supero-temporal semi-meridian. The small-angle diffraction pattern from cornea (Figure 3a) contains a well-defined reflection deriving from the lateral short-range order of stromal collagen fibrils (see Meek and Quantock, 2001). The fibrils in a given lamella scatter x-rays at right-angles to the direction of their long-axes, forming two symmetrical diffraction maxima on the detector. A line normal to that joining the two maxima thereby indicates the fibril direction,

while their intensity is proportional to the number of fibrils aligned in that direction. Thus from the distribution of intensity around the reflection we can detect any preferred fibril orientation (over and above any isotropically arranged collagen) and determine the relative number of fibrils oriented in any particular direction within the plane of the cornea (Daxer and Fratzl, 1997; Newton and Meek, 1998b).
Figure 3b shows the intensity of the x-ray scattering plotted as a function of angle round the reflection. The plot consists of two separable components, a contribution from the isotropically aligned fibrils (shown shaded) and a contribution from the preferentially aligned fibrils (shown clear). The peak positions allow us to determine the angles at which the preferentially aligned fibrils are running at the point in the tissue where the x-ray pattern was obtained, and the intensity of the peaks above background gives a relative measure of the amount of collagen running in that direction. By producing plots such as this from all the sampling locations indicated in Figure 2, we were thus able to monitor the size and direction of the two principal fibril populations (centrally, superior-inferior and nasal-temporal) as they change with radial distance from the centre of the cornea.

Results

Figure 4 shows how the preferred directions of the (initially) superior-inferior and nasal-temporal fibril populations change with radial distance from the corneal centre along the two sampling lines. Along the nasal semi-meridian, the directions of the two populations of fibrils remain essentially unchanged and mutually orthogonal from the central cornea up to the limbus about 5mm away (Figure 4(a). However along the supero-temporal semi-meridian (Figure 4b) there is clearly rotation of the preferred fibril angle for the superior-inferior population in order for these fibrils to become tangential at the limbus. In agreement with results obtained by Newton and Meek (1998a) this rotation appears to occur within the cornea in a space of 1-1.5 mm just before the limbus.

The intensities of the peaks in the x-ray scattering plot arising from the preferentially aligned nasal-temporal and inferior-superior fibrils (Figure 3b) are plotted as a function of radial distance from the corneal centre in Figure 5. The data show that in both directions studied, the amount of collagen in the preferentially aligned superior-inferior and nasal-temporal populations remain unchanged until 3-4 mm from the corneal centre and that, furthermore, the two populations are comparable in magnitude over this region. However as we move further away from the corneal centre the amount of collagen in both populations begins to increase, the superior-inferior at a faster rate than the nasal-temporal. By the time we reach the centre of the limbus (radial distance: 5-5.5 mm) the superior-inferior population, which now run tangentially, are considerably more abundant.

From the total scattering intensity distributions for each of our sampling points we were also able to measure the scattering intensity due to only the isotropically arranged collagen (Figure 3) at that position in the cornea. These data are shown in Figure 6. In both directions studied, the isotropic scatter increases near the limbus, at about the same place that the preferentialy aligned fibril scatter increases.

Discussion

By following the angle between the two preferred orientations of the lamellae along the nasal semi-meridian at very closely spaced intervals, we have shown that nasally, there is little or no change in the preferred lamellar directions (Figure 4a). There is an increase in scattering from the superior-inferior lamellae just before the limbus, suggesting an increase in the number of fibrils in this direction at this point (Figure 5a). At the nasal limbus, these are lamellae running tangentially to the cornea and could arise from bending of lamellae previously running in other directions, or by additional aligned material in the peripheral cornea reinforcing the fibrils from the corneal centre. In the former situation, the increased thickness of the peripheral cornea would need to be accounted for elsewhere, possibly from the additional non-aligned collagen near the limbus (Figure 6a). Similarly, there is no change in the direction of the nasal-temporal fibrils (Figure 4a). However, these fibrils are reinforced near the limbus (Figure 5a) and bearing in mind that this scattering comes from radial fibrils, the question arises as to where additional radial fibrils could come

from near the edge of the cornea. We suggest that this reinforcement comes from fibrils that have curved into the nasal-temporal direction from elsewhere.

In the supero-temporal semi-meridian, there is also no change in the direction of the nasal-temporal fibrils (Figure 4b), but they are reinforced by other fibrils (Figure 5b). Again, this suggests that lamellae have curved to reinforce the nasal-temporal fibrils near the limbus. But the most striking observation is that the angle of the superior-inferior fibrils changes gradually when approaching the supero-temporal limbus (Figure 4b). This is perhaps the most compelling evidence that these lamellae must curve to become tangential at the limbus.

The data we have presented here help to explain how the predominantly orthogonal fibrils of the central cornea might integrate with those in the circum-corneal annulus, by reducing the problem to a consideration of the numbers and directions of the three principal central fibril populations: superior-inferior, nasal-temporal and isotropic. While clearly this is a somewhat simplistic view of the cornea, based on the current data, it seems very unlikely that the limbal annulus consists of a separate population of tangential/circular fibrils (Figures 1a and 1b). Such a scenario would show up as a much more abrupt, discontinuous change in fibril alignment near the limbus. Furthermore, it is difficult to explain the reinforcement of the nasal-temporal lamellae as we approach the limbus using a model where lamellae do not change direction. So, even though our measurements do not follow the individual fibrils/lamellae, our data can best be understood in terms of a combination of lamellae bending just before the limbus (Figure 1d) and additional collagen anchored in the sclera crossing the peripheral cornea – at least some of which must follow a curved path (Figure 1c). This bending could be achieved by a combination of lamellae splitting and then fusing with lamellae running at a different angle, as suggested by the work of Radner et al. (1998). However, our data also indicate that there is some difference in the transition from cornea to sclera depending on which part of the limbus is being examined (compare Figures 5a and 5b), so the manner of integration is not circularly symmetrical as shown in Figure 1.

The collagen in the cornea plays an important role both at the microscopic level, where it allows the tissue to maintain its transparency, and also at the macroscopic level, where it confers shape and strength. At the microscopic level we still do not know the precise manner in which collagen molecules pack together to form fibrils, how many intermediate levels there are in the structural heirarchy and how different collagens associate with each other and with other matrix components. Similarly, questions remain at the macroscopic level. Clearly, the precise manner in which the cornea, limbus and sclera fuse is complex and far from understood. However, from detailed studies such as those described here, we intend to examine other positions around the cornea, and to investigate how lamellae in the peripheral cornea and limbus are arranged as a function of tissue depth.

Acknowledgements.

The authors would like to thank Dr. Christian Riekel and Dr Manfred Burghammer at the European Synchrotron Radiation Facility and Dr. Andrew Quantock and Dr. Hossein Aghamohammadzadeh at Cardiff University for help in collecting the x-ray data. This work was funded by the Wellcome Trust and the Medical Research Council.

References

Baldock, C., Gilpin, C.J., Koster, A.J., Ziese, U., Kadler, K.E., Kielty, C.M. and Holmes, D.F. (2002) Three-dimensional reconstructions of extracellular matrix polymers using automated electron tomography. J. Struct. Biol. 138, 130-136.

Birk, D.E., Finch, J.M. and Linsenmayer, T.F. (1986) Organization of collagen Types I and V in the embryonic chicken cornea. Invest. Ophthalmol. Vis. Sci. 27, 1470-1477.

Boote, C., Dennis, S., Newton, R.H., Puri, H. and Meek, K.M. (2003) Collagen fibrils appear more closely packed in the prepupillary cornea: optical and biomechanical implications. Invest. Ophthalmol. Vis. Sci. 44, 2941-2948.

Boote, C., Dennis, S and Meek, K.M. (2003) Collagen organisation in adult and foetal marmoset cornea. Invest. Ophthalmol. Vis. Sci. 44: ARVO E-Abstract 884.

Borcherding, M.S., Blacik, I.J., Sittig, R.A., Bizzell, J.W., Breen, M. and Weinstein, H.G. (1975) Proteoglycans and collagen fibre organisation in human corneoscleral tissue. Exp. Eye Res. 21, 59-70.

Bron, A.J. (2001) The architecture of the corneal stroma. Br. J. Ophthalmol. 85, 379-383.

Chakravarti , Magnuson, T., Lass, J.H., Jepsen, K.J., LaMantia, C. and Carroll, H. (1998). Lumican regulates collagen fibril assembly: Skin fragility and corneal opacity in the absence of lumican. J Cell Biol. 141:1277-1286.

Chakravarti S, Petroll, W.M., Hassell., (2000) Corneal opacity in lumican-null mice: Defects in collagen fibril structure and packing in the posterior stroma. *Invest Ophthalmol Vis Sci*.41, 3365-3373.

Cintron, C., Hong, B.-S. and Covington, H.I. (1988) Heterogeneity of collagens in rabbit corneas: Type III collagen. Invest. Ophthalmol. Vis. Sci. 29, 767-775.

Craig, A.S., Robertson, J.G., Parry, D.A. (1986) Preservation of corneal fibril structure using low-temperature procedures for electron microscopy. J. Ultrastructure Mol. Struct. Res. 96, 172-175.

Danielson KG, Baribault H, Holmes DF, Graham H, Kadler KE, Iozzo RV.(1997) Targeted disruption of decorin leads to abnormal collagen fibril morphology and skin fragility. J Cell Biol ,136:729-743.

Davison, P.F., Hong,B.S. and Cannon, D.J. (1979) Quantitative analysis of the collagens in the bovine cornea. Exp. Eye Res. 29, 97-107.

Daxer, A. and Fratzl, P. (1997) Collagen fibril orientation in the human corneal stroma and its implicatins in keratoconus. Invest. Ophthalmol. Vis. Sci. 38, 121-129

Daxer, A., Misof, K., Grabner, B., Ettl, A. and Fratzl, P. (1998) Collagen fibrils in the human corneal stroma: structure and aging. Invest. Ophthalmol. Vis. Sci. 39, 644-647.

Eliason, J. and Maurice, D. (1981) Stress distribution across the in vivo human cornea. Invest. Ophthalmol. Vis. Sci. 20 Suppl. (ARVO Abstracts) 156.

Farrell, R.A. and McCally, R.L. (2000) Corneal Transparency. In Principles and practice of ophthalmology (D.M. Albert and F.A. Jakobiec, eds) W.B. Saunders Company, Philadelphia. pp 629-643.

Freund, D.E., McCally, R.L., Farrell, R.A., Crystol, S.M., L'Hernault, N.L. and Edelhauser, H.F. (1995) Ultrastructure in anterior and posterior stroma of erfused human and rabbit corneas. Invest. Ophthalmol. Vis. Sci. 36, 1508-1523.

Fullwood, N.J. and Meek, K.M. (1993) A synchrotron X-ray study of the changes occurring in the corneal stroma during processing for electron microscopy. J. Microsc. 169, 53-60.

Goodfellow, J.M., Elliott, G.F. and Woolgar, A.E. (1978) X-ray diffraction studies of the corneal stroma. J. Mol. Biol. 119, 237-252.

Gyi, T.J., Meek, K.M. and Elliott, G.F. (1988). Collagen interfibrillar distances in corneal stroma using synchrotron X-ray diffraction: A species study. Int. J. Biol. Macromol., 10, 265-269.

Hamada, R., Giraud, J.P., Graf, B. and Pouliquen, Y. (1972) Analytical and statistical study of the lamellae, keratocytes and collagen fibrils of the central region of the normal human cornea. Arch. D'Ophtalmologie et Revue Generale d'Ophtalmologie. 32, 563-570.

Kanai, A. and Kaufman, H.E. (1973) Electron microscopic studies of corneal stroma: aging changes of collagen fibers. Annals Ophthalmol. 5, 285-287.

Keene, D.R., Sakai, L.Y., Bächinger, H.P. and Burgeson, R.E. (1987) Type III collagen can be present on banded collagen fibrils regardless of fibril diameter. J. Cell Biol. 105, 2393-2402.

Kokott, W. (1938) Übermechanisch-funktionelle Strikturen des Auges. Albrecht von Graefes Arch. Ophthal. 138, 424-485

Komai, Y. and Ushiki, T. (1991) The three-dimensional organisation of collagen fibrils in the human cornea and sclera. Invest. Ophthalmol. Vis. Sci. 32, 2244-2258.

Kostyuk O, Nalovina O, Mubard TM, Regini, JW, Meek, KM, Quantock, AJ, Elliott, GF and Hodson SA (2002) Transparency of the bovine corneal stroma at physiological hydration and its dependence on concentration of the ambient ion. J. Physiol. 543.2 633-642.

Linsenmayer, T.F., Bruns, R.R., Mentzer, A. and Mayne, R. (1986) Type VI collagen:immunohistochemical identification as a filamentous component of the extracellular matrix of the developing avian corneal stroma. Devel. Biol. 118, 425-431.

Löpping, B. and Weale, R.A. (1965) Changes in corneal curvature following ocular convergence. Vision Res., 5, 207-215.

Malik, NS, Moss,SJ, Ahmed, N, Furth, AJ, Wall, RS and Meek, KM (1992) Ageing of the human corneal stroma: structural and biochemical changes. Biochim. Biophys. Acta. 1138, 222-228.

Marin_Amat, M. (1956) Les variations physiologiques de la courbure de la corneé pendant de vie. Leur importance et transcendance dans la refraction oculaire. Bull. Soc. belge Ophthal., 113, 251-293.

Marshall, G.E., Konstas, A.G. and Lee, W.R. (1991) Immunogold fine structural localization of extracellular matrix components in aged human cornea. 1. Types I-IV collagen and laminin. Graefe's Arch. Clin. Exp. Ophthalmol. 229, 157-163.

Maurice, D.M. (1957) The structure and transparency of the cornea. J. Physiol. 136, 263-286

Maurice DM. (1969) The Cornea and Sclera. Davson H. *The Eye*. New York: Academic Press; 489-599.

Maurice, D.M. (1984) The cornea and sclera. In The Eye (ed. H. Davson) Academic Press, Orlando, Fl.

Maurice, D.M. (1988) Mechanics of the cornea. In The Cornea: Transactions of the World Congress on the Cornea III (ed H. Dwight Cavanagh). Raven Press Ltd., New York.

McPhee, T.J., Bourne, W.M. and Brubaker, R.F. (1985) Location of the stress-bearing layers of the cornea. Invest. Ophthalmol. Vis. Sci. **XXX**, 869-872.

Meek, K.M. and Holmes, D.F. (1983). Interpretation of the electron microscopical appearance of collagen fibrils from corneal stroma. Int. J. Biol. Macromol., 5, 17-25

Meek, K.M. and Leonard, D.W. (1993) Ultrastructure of the corneal stroma: a comparative study. Biophys. J. 64, 273-280.

Meek, K.M. and Fullwood, N.J. (2001) Corneal and scleral collagens – a microscopist's perspective. Micron 32, 261-272.

Meek, K.M. and Quantock, A.J. (2001) The use of X-ray scattering techniques to determine corneal ultrastructure. Prog. Ret. Eye Res. 20 95-137

Meek, K.M., Elliott, G.F. and Nave, C. (1986) A synchrotron x-ray diffraction study of bovine cornea stained with cupromeronic blue. Collagen Res. Rel. 6, 203-218.

Meek, K.M., Blamires, T., Elliott, G.F., Gyi, T.J. and Nave, C. (1987). The organisation of collagen fibrils in the human corneal stroma: A synchrotron X-ray diffraction study. Current Eye Research, 6, 841-846

Müller, L.J., Pels, E. and Vrensen, G.F.J.M. (2001) The specific architecture of the anterior stroma accounts for maintenance of corneal curvature. Br. J. Ophthalmol. 85, 437-443.

Nakamura, M., Kimura, S., Kobayashi, M. Hirano, K., Hoshino, T. and Awaya, S. (1997) Type VI collagen bound to collagen fibrils by chondroitin/dermatan sulphate glycosaminoglycan in mouse corneal stroma. Jpn. J. Ophthalmol. 41, 71-76.

Newton, R.H. and Meek, K.M. (1998a) The integration of the corneal and limbal fibrils in the human eye. Biophys. J. 75, 2508-2512.

Newton, R.H. and Meek, K.M. (1998b) Circum-corneal annulus of collagen fibrils in the human limbus. Invest. Ophthalmol. Vis. Sci. 39, 1125-1134.

Polack, F.M. (1961) Morphology of the cornea. I. Study with silver stains. Am J. Ophthalmol. 51, 1051-1056.

Praus, R., Brettschneider, I. and Adam, M. (1979) Heterogeneity of the bovine corneal collagen. Exp. Eye Res. 29, 469-477.

Rada, J.A., Cornuet, P.K. and Hassell, J.R. (1993) Regulation of corneal fibrillogenesis in vitro by corneal proteoglycan (lumican and decorin) core proteins. Exp. Eye Res. 56, 648-653.

Radner, W., Zehetmayer, M., Mallinger, M. and Kulnig W (1993) Zur dreidimensionalen Anordnung der bkollagenen Lamellen im posterioren Stroma der menschlichen Hornhaut. Spektrum Augenheilkd, 7, 77-80

Radner, W., Zehetmayer, M., Aufreiter, R. and Mallinger, R. (1998) Interlacing and cross-angle distribution of collagen lamellae in the human cornea. Cornea 17, 537-543.

Sayers, Z., Whitburn, S.B., Koch, M.H.J., Meek, K.M. and Elliott , G.F.(1982). Synchrotron X-ray diffraction study of corneal stroma. J Mol. Biol., 160, 593-607

Scott, J.E. and Haigh, M. (1988) Identification of specific binding sites for keratan sulphate proteoglycans and chondroitin-dermatan sulphate proteoglycans on collagen fibrils in cornea by the use of cupromeronic blue in critical electrolyte concentration techniques. Biochem. J. 253, 607-610.

Scott, J.E. and Orford, C.R. (1981) Dermatan sulphate-rich proteoglycan associates with rat tail tendon at the d-band in the gap region. Biochem. J. 197, 213-216.

Scott, J.E. and Thomlinson, A.M. (1998) The structure of interfibrillar protein bridges (shape modules) in extracellular matrix of fibrous connective tissues and their stability in various chemical environments. J. Anat. 192, 391-405.

Wall, R,S. and Gyi, T.S. (1988) Alcian blue staining of proteoglycans in polyacrylamide gels using the "critical electrolyte concentration" approach.
Anal Biochem.175:298-299.

Wessel, H., Anderson, S., Fite, D., Halvas, E., Hempel, J. and SundarRaj, N. (1997) Type XII collagen contributes to diversities in human corneal and limbal extracellular matrices. Invest. Ophthalmol. Vis. Sci. 38, 2408-2422.

Worthington, C.R. and Inouye, H. (1985) X-ray diffraction study of the cornea. Int. J. Biol. Macromol. 7, 2-8

Zimmerman, D.R., Trüeb, B., Winterhalter, K.H., Witmer, R. and Fischer, R.W. (1986) Type VI collagen is a major component of the human cornea. FEBS Letters, 197, 55-58

Legends to Figures

Figure 1
Schematic diagrams showing four possible arrangements of the integration between the preferentially aligned collagen (lamellae) in the central human cornea (inferior-superior and nasal-temporal) and in the limbus (tangential). In (a) there are two separate populations of fibrils, with the limbal fibrils forming a discrete annulus. In (b) and (c) the collagen at the limbus forms an anchoring network by either running across the limbus tangentially (b) or curving in and out of the limbus (c). In (d) the collagen in the cornea bends near the periphery to form a circular annulus at the limbus.

Figure 2
Position of micro-focus x-ray sampling lines with respect to the cornea (posterior face shown).

Figure 3
(a) The small-angle diffraction pattern from central human cornea features four orthogonal intensity peaks, indicating two predominant fibril populations running superior-inferior and nasal-temporal. (b) Shows total scattered x-ray intensity plotted as a function of angle round the interfibrillar reflection. Scattering may be divided into two separate components: an isotropic component arising from collagen fibrils occuring equally in all directions, and a component deriving entirely from preferentially aligned fibrils.

Figure 4
(a) Preferred direction of (centrally) superior-inferior and nasal temporal fibril populations as a function of distance from the corneal centre along the nasal semi-meridian. (b) Corresponding data for the supero-temporal semi-meridian. We have estimated the maximum error in our absolute radial position on the cornea to be +/- 0.5mm.

Figure 5
(a) Aligned peak scattering intensity value for (centrally) superior-inferior and nasal-temporal fibril populations as a function of distance from the corneal centre along the nasal semi-meridian. (b) Corresponding data for the supero-temporal semi-meridian.

Figure 6
(a) Isotropic collagen scattering intensity as a function of distance from the corneal centre along the nasal semi-meridian. (b) Corresponding data for the supero-temporal semi-meridian.

Figure 1

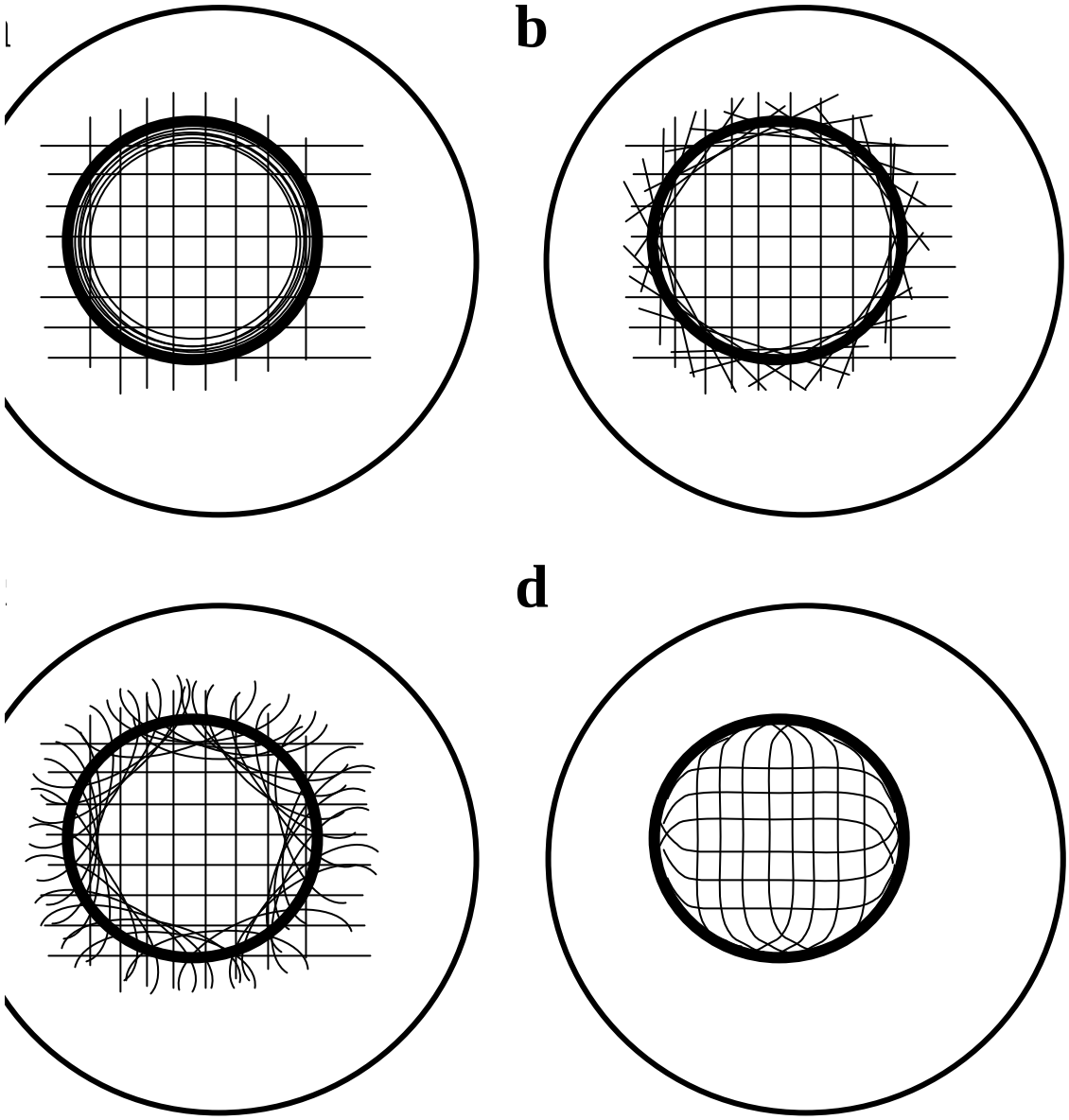

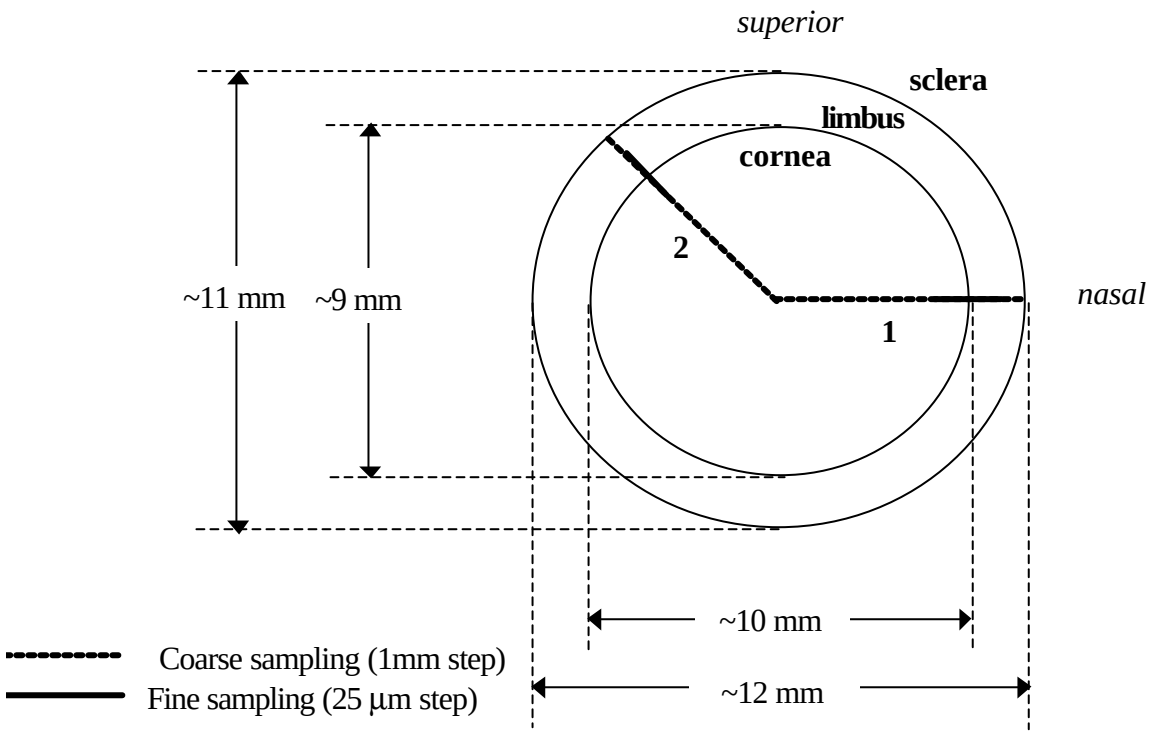
superior
sclera
limbus
cornea
2
1
nasal
~11 mm
~9 mm
~10 mm
~12 mm
Coarse sampling (1mm step)
Fine sampling (25 µm step)

Figure 2

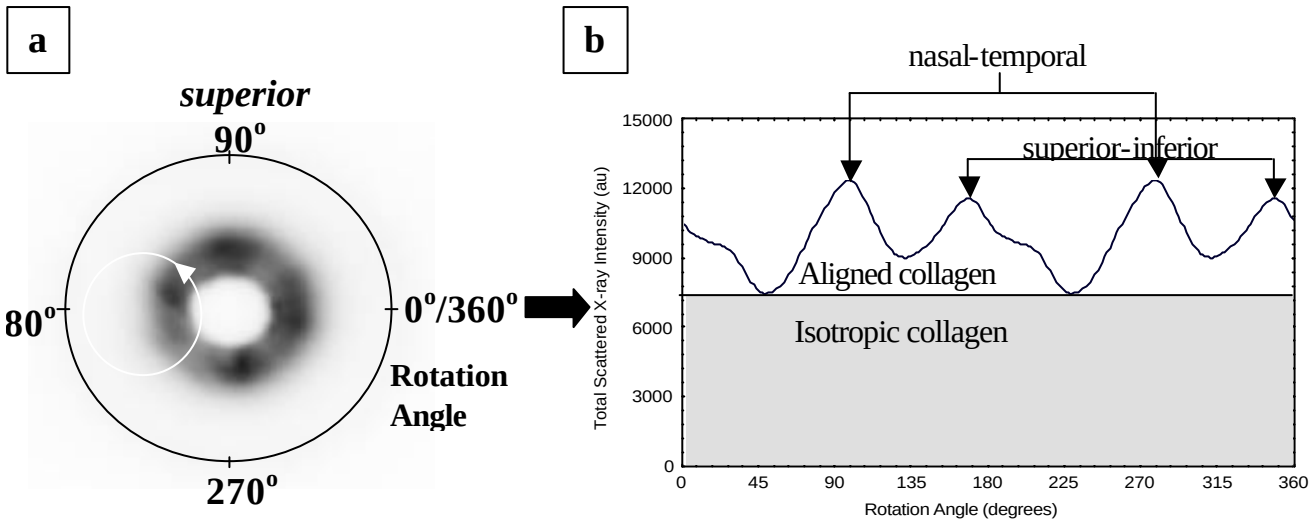
a
superior
90°
80°
0°/360°
270°
Rotation
Angle
b
nasal-temporal
superior-inferior
Aligned collagen
Isotropic collagen
Total Scattered X-ray Intensity (au)
15000
12000
9000
6000
3000
0
0
45
90
135
180
225
270
315
360
Rotation Angle (degrees)

Figure 3

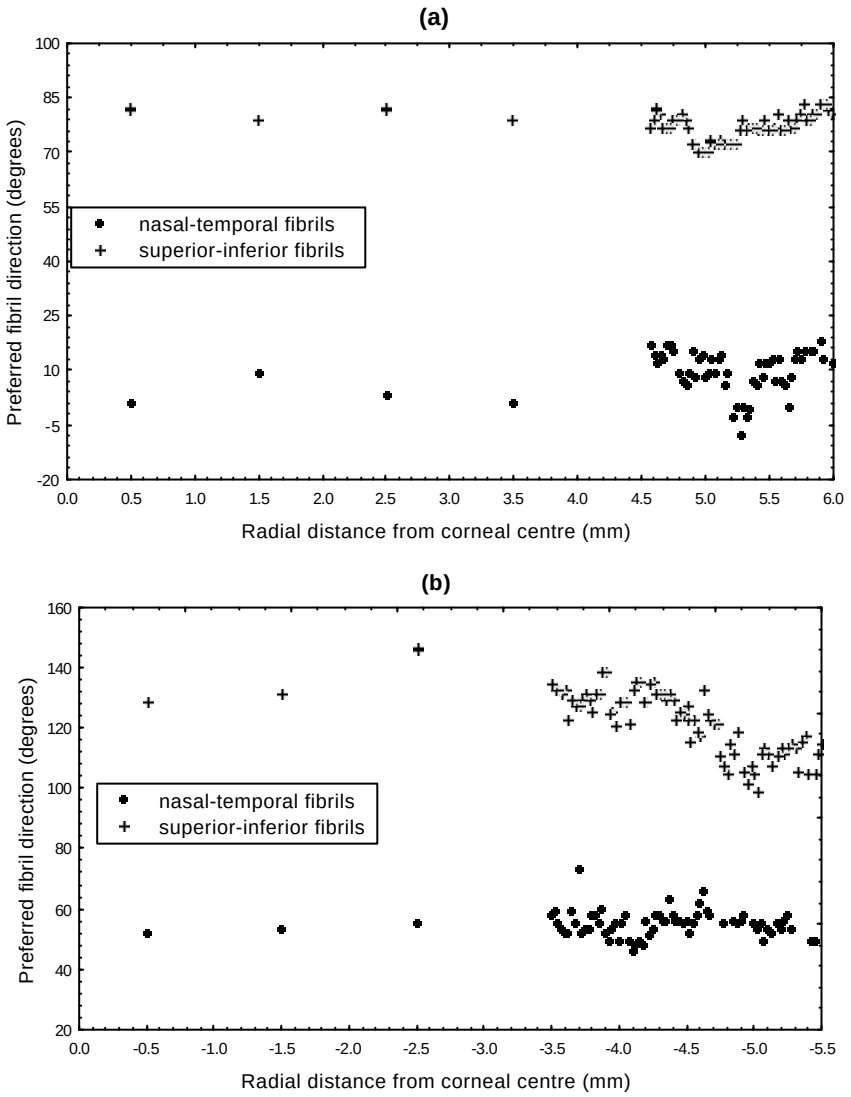
(a)
Preferred fibril direction (degrees)
100
85
70
55
40
25
10
-5
-20
nasal-temporal fibrils
superior-inferior fibrils
0.0
0.5
1.0
1.5
2.0
2.5
3.0
3.5
4.0
4.5
5.0
5.5
6.0
Radial distance from corneal centre (mm)
(b)
Preferred fibril direction (degrees)
160
140
120
100
80
60
40
20
nasal-temporal fibrils
superior-inferior fibrils
0.0
-0.5
-1.0
-1.5
-2.0
-2.5
-3.0
-3.5
-4.0
-4.5
-5.0
-5.5
Radial distance from corneal centre (mm)

Figure 4

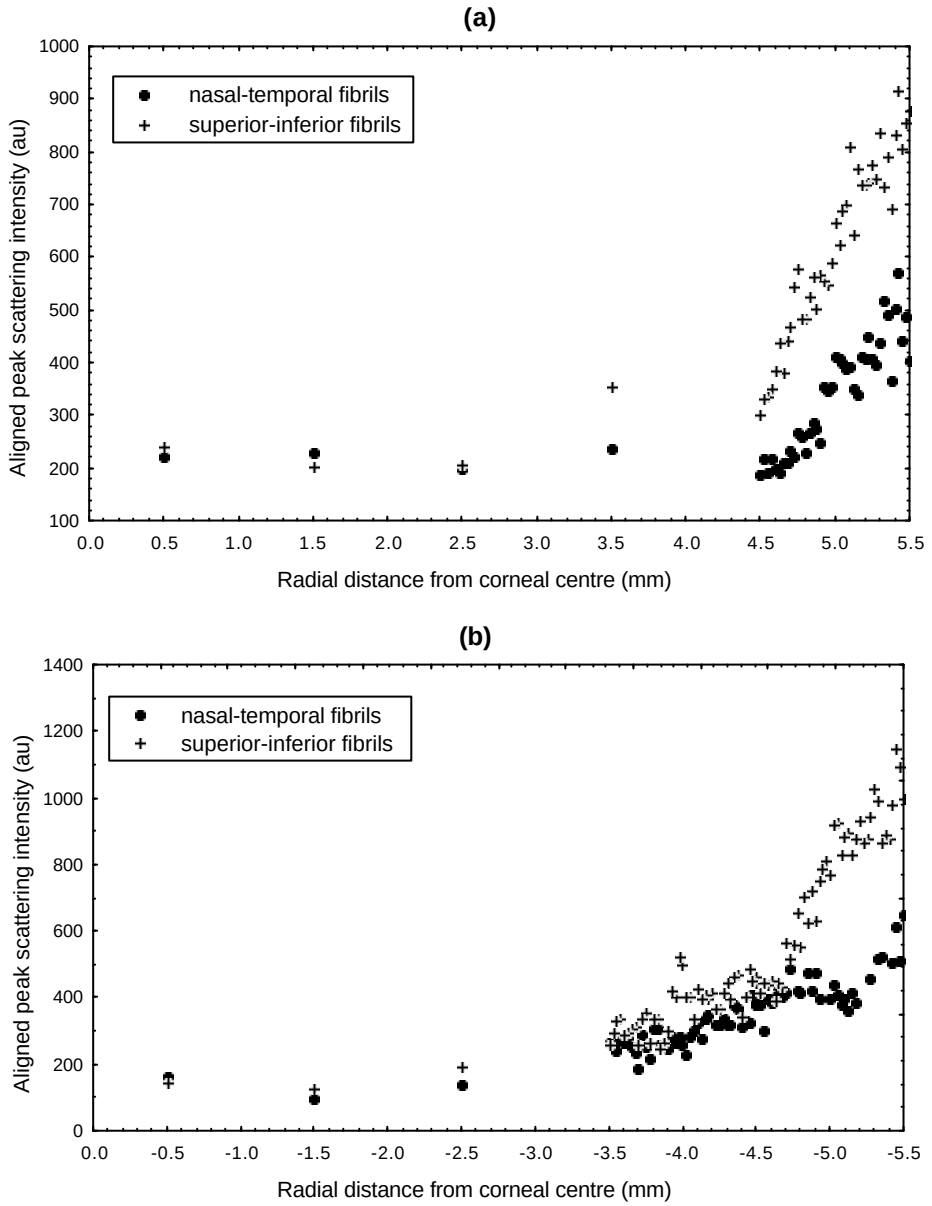
(a)
nasal-temporal fibrils
superior-inferior fibrils
Aligned peak scattering intensity (au)
Radial distance from corneal centre (mm)
(b)
nasal-temporal fibrils
superior-inferior fibrils
Aligned peak scattering intensity (au)
Radial distance from corneal centre (mm)

Figure 5

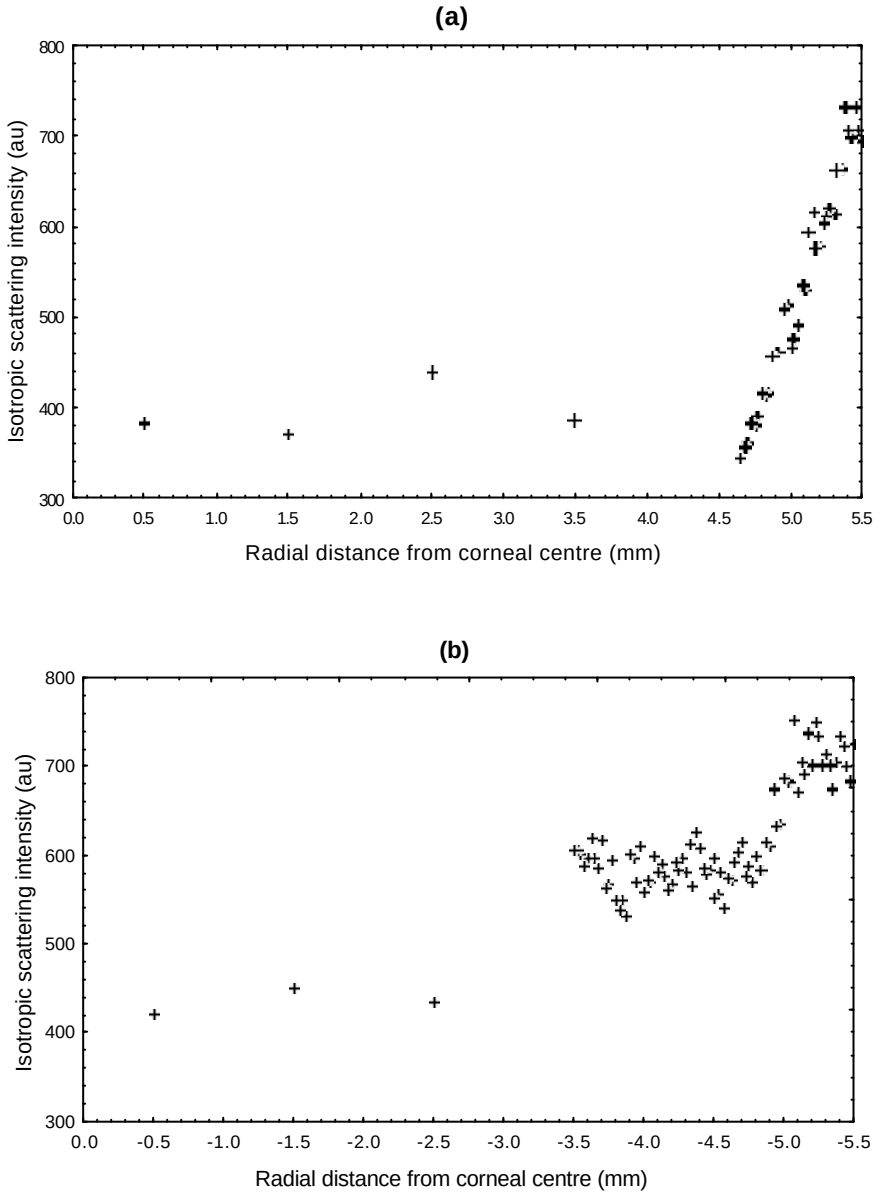
(a)
Isotropic scattering intensity (au)
800
700
600
500
400
300
0.0
0.5
1.0
1.5
2.0
2.5
3.0
3.5
4.0
4.5
5.0
5.5
Radial distance from corneal centre (mm)
(b)
Isotropic scattering intensity (au)
800
700
600
500
400
300
0.0
-0.5
-1.0
-1.5
-2.0
-2.5
-3.0
-3.5
-4.0
-4.5
-5.0
-5.5
Radial distance from corneal centre (mm)

Figure 6